Available online at www.sciencedirect.com
ScienceDirect
European Journal of Protistology 44 (2008) 181–196
European Journal of PROTISTOLOGY
www.elsevier.de/ejop

Redescription of *Cardiosporidium cionae* (Van Gaver and Stephan, 1907) (Apicomplexa: Piroplasmida), a plasmodial parasite of ascidian haemocytes

A. Ciancio[a,*], S. Scippa[b,d], M. Finetti-Sialer[c], A. De Candia[b], B. Avallone[b], M. De Vincentiis[b,d]

[a]*CNR, Istituto per la Protezione delle Piante, Via Amendola 122/D, I-70126 Bari, Italy*
[b]*Dipartimento delle Scienze Biologiche, Sezione di Genetica e Biologia Molecolare, Facoltà di Scienze, Università di Napoli "Federico II", Via Mezzocannone 8, 80134 Napoli, Italy*
[c]*Dipartimento Protezione Piante e Microbiologia Applicata, Università degli Studi, Bari, Italy*
[d]*Stazione Zoologica "Anton Dohrn", Napoli, Italy*

Received 8 August 2007; received in revised form 19 November 2007; accepted 24 November 2007

Abstract

Cardiosporidium cionae (Apicomplexa), from the ascidian *Ciona intestinalis* L., is redescribed with novel ultrastructural, phylogenetic and prevalence data. Ultrastructural analysis of specimens of *C. intestinalis* collected from the Gulf of Naples showed sporonts and plasmodia of *C. cionae* within the host pericardial body. Several merogonic stages and free merozoites were found in the pericardial body, together with sexual stages. All stages showed typical apicomplexan cell organelles, i.e. apicoplasts, rhoptries and subpellicular microtubules. Merogonic stages of *C. cionae* were also produced inside haemocytes. A fragment of the rSSU gene of *C. cionae* was amplified by PCR using DNA extracted from the pericardial bodies. The amplified product showed closest affinity with other apicomplexan representatives and a 66 bp unique insertion, specific for *C. cionae*, at position 1644. Neighbour-joining phylogenetic analysis placed *C. cionae* in a clade with other piroplasm genera, including *Cytauxzoon*, *Babesia* and *Theileria* spp. The parasite was found in different populations of *C. intestinalis* with highest prevalence in October–November. Ultrastructural and DNA data showed that the organism, described in 1907 from the same host but not illustrated in detail, is a member of a novel marine apicomplexan radiation of tunicate parasites.

Keywords: Apicomplexa; Ascidians; Piroplasmida; *Cardiosporidium*; Pericardial body; Sporogony

Introduction

A species of eukaryotic parasite, *Cardiosporidium cionae* Van Gaver and Stephan, was described in 1907 as a "sporozoan" infecting the ascidian *Ciona intestinalis* L. (Van Gaver and Stephan 1907). In the original short report, the parasite was described as a plasmodial sporozoan present in juveniles of *C. intestinalis*, in which non-motile, fusiform bodies were found within the host pericardial cavity. These bodies yielded, in mature *C. intestinalis*, round structures of different size,

*Corresponding author. Fax: +39 080 5929230.
E-mail address: a.ciancio@ba.ipp.cnr.it (A. Ciancio).

0932-4739/$ - see front matter © 2008 Elsevier GmbH. All rights reserved.
doi:10.1016/j.ejop.2007.11.005

embedded within granular masses. They were thought to originate in a mobile mucilaginous mass, known as the pericardial body (Fernandez 1906; Kalk 1970; Roule 1884; Scippa and Izzo 1996). The parasite showed a vacuolar cytoplasm provided with a single, central dark area or surrounded by a series of smaller units, giving rise to a sort of plasmodium. Plasmodia were covered by a membrane with protruding elements (supposed to be spines) and showed several round cells internally, in peripheral areas. The parasite life-cycle appeared asynchronous, as plasmodia were observed at different developmental stages in the pericardial cavity. Two types of reproductive cells were also reported: the first one with a round shape, bearing an elongated self-replicated cell provided with a small ''plaque'' on its convex side, whereas the second type was a mobile, pyriform cell provided with two flagella (Van Gaver and Stephan 1907).

The parasite was associated with the ascidian pericardial body, a globular formation occurring inside the empty space surrounding the heart, known as the pericardial cavity. The nature and origins of this structure were investigated in *C. intestinalis* and other species of ascidians (Fernandez 1906; Kalk 1970; Roule 1884; Scippa and Izzo 1996). It appears as a fibrous, amorphous matrix, subject to continuous oscillations due to pulsations of the heart. Cells of different size and origins (i.e. degenerated blood cells and, in lower numbers, lymphocyte-like blood cells or degenerated cardiac fibers), derived from the blood or the pericardial epithelium, were observed inside this matrix (Fernandez 1906; Kalk 1970; Millar 1953; Roule 1884). In a transmission electron microscopy (TEM) study of *C. intestinalis*, all blood cell types were found within this formation (Scippa and Izzo 1996).

The original description of *C. cionae* by Van Gaver and Stephan was based on direct observations of fresh squashes of pericardial bodies and on Giemsa- or hematoxylin-stained material. However, the description was far from complete, since, although reporting some life-stages, it was not integrated by any detailed illustrations. Considering that modern criteria for species assignation among Apicomplexa (the modern Phylum including some of the former ''sporozoans'') require evidence from DNA and/or ultrastructural data, we considered it necessary to enlarge and revise the original description of *C. cionae*. No reference to this organism or emended description was made in the years after its description, apart from a citation by Ormières (1964). In a recent study of this species, caused by its re-discovery in specimens during ultrastructural studies of *C. intestinalis* haemocytes, some ultrastructural data were presented. The organism was partially illustrated with TEM and a first discussion about its putative taxonomic position was also provided (Scippa et al. 2000). TEM data showed its eukaryotic position, some stages of a complex life-cycle, including plasmodial or sporogonic stages and merozoites, sporozoites and/or sexual stages, proposing a possible link with the Hemosporina, the order including *Plasmodium* spp. and other blood parasites (Scippa et al. 2000). *C. cionae* was later observed from specimens of *C. intestinalis* collected in other coastal areas of Naples, and always appeared in squashes of their pericardial bodies.

Further literature reports from other ascidian species also provided convincing evidence about the occurrence of unknown microparasites in blood cells of Tunicata (Choi et al. 2006). Tunicate blood may hence represent a specific trophic niche for cryptic parasites, and observations suggest the putative occurrence of new evolutionary radiations of apicomplexans. This view is also supported by the recent reappraisal of a darwinian hypothesis considering Tunicata as simplified chordates, rather than as the organisms closest to chordate ancestors (Chourrout et al. 2006). The location of plasmodial stages, the infective propagative stages and the life-cycle of *C. cionae* within the host tissues are still unknown, as are its mode of transmission and the route of invasion. In this paper we provide more data on *C. cionae* and, on the basis of further observations on the ultrastructure of plasmodial stages, on ribosomal DNA sequence data and prevalence, we revise the status of this organism as a piroplasm member of Apicomplexa.

Materials and methods

Light microscopy and prevalence studies

Specimens of *C. intestinalis* were collected in shallow waters at Castellammare di Stabia (Naples) and Lago Fusaro, a close coastal marsh. For light microscopy (LM), the pericardial bodies were removed after incision of the hearts and after squashing were observed with interference contrast microscopy (Polivar Reichert). Other pericardial bodies were pre-fixed in 4% glutaraldehyde, 0.2 M Na cacodylate (pH 7.2), 5 mM $CaCl_2$, 0.35 M sucrose, 0.05% OsO_4 for 10 min at 4 °C, washed in the same buffer and fixed in the same medium as used for pre-fixing, but without OsO_4, for 1 h at room temperature, according to the method of Eisenman and Alfert (1982) and McDonald (1984). These samples were then washed again in the same buffer, and post-fixed in 1% OsO_4, 0.8% $K_3Fe(CN)_6$, and Na cacodylate (pH 7.2) for 1 h in the dark. Following this treatment, the specimens were washed in the same buffer and then in bidistilled water and 1% aqueous uranyl acetate for 1 h in the dark. The specimens were then dehydrated in a graded ethanol series followed by treatment with propylene oxide and embedding in Epon. Semi-thin sections (2 μm) were stained with toluidine blue as described by Scippa et al. (2000).

A simple staining method, aiming at the detection and identification of *C. cionae* nuclear material in plasmodial and/or other sporogonic stages, was devised. Several pericardial bodies were fixed for 5 min in pure methanol or in an ether–methanol series (95–40%) for 5 min at each step. Two different stains were used. The first was not specific and based on Giemsa (Kawamoto 1991; Mpoke and Wolfe 1997; Payne 1988), whereas the second, more specific, was based on acridine orange (AO). The latter is a DNA-selective stain, fluorescing at 525 nm when intercalated, and is useful in cell cycle studies discriminating between quiescent, active and proliferating cells (Darzynkiewicz 1990; Darzynkiewicz and Kapuscinski 1990).

For Giemsa staining, the smears of the pericardial bodies were stained on a slide for 15–60 min after fixation, by adding a few drops of a 5% (v/v) diluted Giemsa solution in sterile distilled water (SDW, pH 7.2). Alternatively, the pericardial bodies were stained by immersion for 30–45 min in 3% Giemsa solution in SDW and smeared. The slides were then washed, air dried and observed with light microscopy at 40 × or at 100 × with an oil immersion objective, for identification of plasmodial stages. Staining with AO was performed after fixing the smears for 15 min in 95% methanol–ether solution (50:50, v/v), followed by hydration through a graded ethanol series. The samples were then rinsed in SDW, immersed in 1% acetic acid, rinsed again in SDW and stained for 3 min in a 10% AO solution in phosphate buffer (PB). The samples were cleared for 1 min in PB and then differentiated for 30 s in $CaCl_2$, washed again in PB and mounted for examination by epifluorescence with a fluorescence microscope (Nikon Eclipse E 1000) equipped with a FITC (fluorescein isothiocyanate) filter (excitation: 465–495 nm; DM: 505 nm; BA: 515–555 nm). Smears of untreated pericardial bodies were also used as controls through examination in light transmission mode.

For prevalence estimation, pericardial bodies were extracted from samples of *C. intestinalis*, each of 4–13 specimens, collected at 1- to 2-week intervals during October and November. The pericardial bodies were stained and examined as described with LM, in order to identify one or more life-stages of the parasite.

Ultrastructure

For TEM, the pericardial bodies were fixed by the methods of Eisenman and Alfert (1982) and McDonald (1984), stained and embedded in Epon, as described above. Ultra-thin sections were cut with a diamond knife. The sections were stained with uranyl acetate and lead citrate and examined using a Siemens Elmiskop 101 TEM.

DNA extraction and amplification

Pericardial bodies were collected from specimens dissected under a stereoscope and stored at 4 °C until used. For DNA extraction, the pericardial bodies were disaggregated using a lysis solution (100 mM Tris, pH 8.5; 100 mM NaCl; 50 mM EDTA; 1% SDS; 1% β-mercaptoethanol; 100 μg/ml Proteinase K). The pellet was then suspended in 500 μl of lysis solution, frozen at −80 °C for 30 min and then incubated for 30–60 min at 55–65 °C with occasional agitation, transferring the solution to new tubes to release larger debris. To clean up nucleic acids, the solution (500 μl) was extracted with an equal volume of phenol/chloroform, before subsequent chloroform extraction. The DNA was precipitated by adding 2.5 vol. ethanol to the final aqueous phase, pelletting the nucleic acids by centrifugation for 10 min at 16,000*g*, washing the pellet with 70% ethanol twice and resuspending the DNA in 50–100 μl Tris/EDTA (10:1).

For PCR amplification, the cycles were run on a thermal cycler in 50 μl buffer mixture using 5 μl of the template DNA suspensions. The PCR buffer was: Taq buffer 1 ×, $MgCl_2$ 1.5 mM, primers 0.5 pmol/μl, dNTP 0.2 mM each, 2.5 units of Taq polymerase (Roche). The amplification cycles included initial denaturing at 95 °C (2 min) and then 35 cycles of denaturing at 92 °C (45 s), annealing at 45 °C (45 s) and extension at 72 °C (1.5 min). The cycles were followed by a last extension step at 72 °C (5 min). Controls included the same mixtures without template with SDW only.

The universal eukaryotic primers used for amplification of the nuclear small ribosomal subunit (rSSU) were 5′-CGAATTCAACCTGGTTGATCCTGCCAGT-3′ (forward) and 5′-CCGGATCCTGATCCTTCTGCAG GTTCACCTAC-3′ (reverse), yielding a total amplified product of approximately 1800 bp (Leander et al. 2003a). For cloning, the amplified fragment was inserted in pGemT and used to transform DH5α competent cells. The recombinant plasmids were sequenced with SP6 and T7 primers through an available commercial service (MWG, Germany). To complete the sequence, the primer 5′-GCTGTACTTCATTGTTACGGTA-3′ (forward) was also used.

Phylogenetic analysis

The programs Bioedit (Hall 1999) and Clustal W (Thompson et al. 1994) were used to align the amplified product to the nearest sequences identified through BLAST analysis (fragment nucleotide identity higher than 90%) that are available in the GenBank NCBI database. To avoid biased taxon sampling, the alignment was integrated with sequences representative of other Apicomplexa or taxa closely related to this phylum, and

listed in the phylogenetic studies of Leander et al. (2003c) and Kopečná et al. (2006). The species and accessions used in this study are given in Fig. 10, and included accessions AF238264, AF238265 and AF238266, derived from uncultured coral reef endosymbionts. The 70-entry alignment was used to infer the phylogenetic position of the sequenced product, using the Neighbour-joining method (Saitou and Nei 1987) with the Kimura or the Jukes and Cantor substitution per site calculations (Jukes and Cantor 1969; Kimura 1980). The distance data

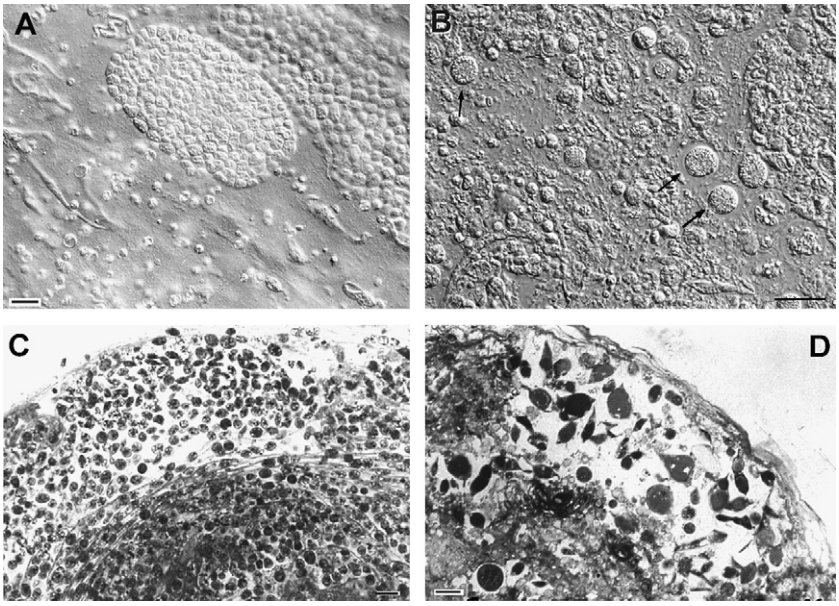

Fig. 1. Light microscope images of *Cardiosporidium cionae*. Plasmodial stages from squashes of pericardial bodies of the tunicate *Ciona intestinalis* in an aggregated cluster (A) and plasmodia free among cell debris (B, arrows). Toluidine blue stained semi-thin sections of pericardial bodies showing large numbers of *C. cionae* merogonic stages (C) and fusiform plasmodia (D). Scale bars: A, B = 20 μm; C, D = 15 μm.

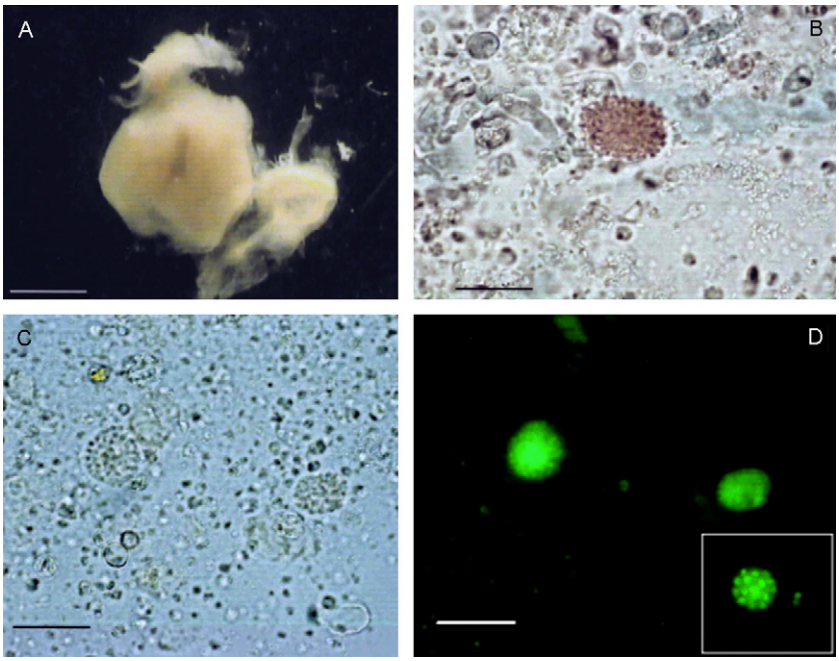

Fig. 2. Pericardial body (A) of the ascidian *Ciona intestinalis*; cells of *Cardiosporidium cionae* stained with Giemsa in (B); plasmodia stained with acridine orange in transmitted light microscopy (C) and in epifluorescence (D, same field as C), showing plasmodial fluorescence and cleaving merozoites surrounding the plasmodial core (D, inset). Scale bars: A = 1 mm; B–D = 20 μm.

matrix was bootstrap resampled 100 times (Felsenstein 1985), with sequence AF368524 (*Zoophthora anglica*) used as outgroup. The software Treecon (Van de Peer and De Wachter 1997) was used to construct and display the corresponding tree.

Results

Light microscopy

Several plasmodia were observed with LM by interference contrast in fresh squashes (Fig. 1A and B) and in semi-thin sections of the pericardial bodies of *C. intestinalis* (Fig. 1C and D). The plasmodia measured $13.5 \pm 3.8\,\mu m$ (mean $\pm$ S.D.) in diameter and were recognized by their morphology; they were present in large numbers in densely packed clusters (Fig. 1A) or free in the pericardial body squash (Fig. 1B). In some plasmodia, clusters of merozoites were visible within the pansporoblastic membrane. Merozoites ranged in number from 9 to 55 per plasmodium and appeared uniformly disposed around a homogeneous central cleaving sporont. Single merozoites free from plasmodia could not be recognized in unstained material or were visible but scarcely distinguishable from the surrounding matrix of cells and debris.

When examined under UV or in LM, the whole pericardial bodies (Fig. 2A) did not show any endogenous fluorescence in untreated controls. Treatment with

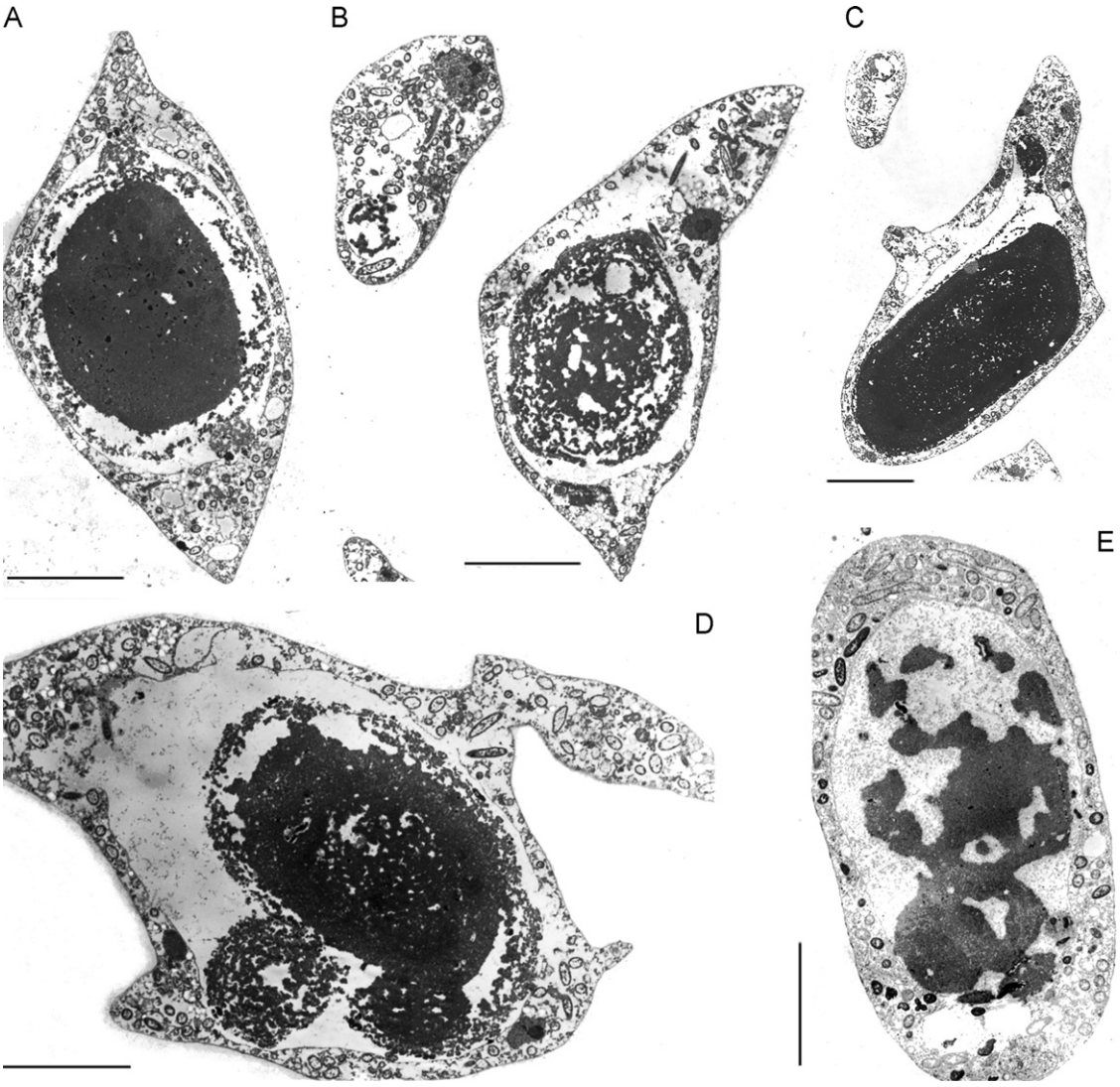

Fig. 3. TEM images of early plasmodial stages of *Cardiosporidium cionae* from pericardial bodies of *Ciona intestinalis*. Plasmodia show elongated and variable fusiform shapes, and possess a central core region containing electron-dense material of differing textures (A–C). At a later stage plasmodia show budding of the central electron-dense core and a more complex structural organization with elongated protrusions (D). A proliferation of putative endosymbiotic bacteria is visible in peripheral areas in B, D, E. Scale bars: A = 3.7 μm; B = 5.8 μm; C = 10 μm; E, D = 5 μm.

Giemsa stained plasmodia red, allowing their identification, but single merozoites were difficult to identify (Fig. 2B). Merozoites and sporozoites were, however, made visible by AO staining, in a reproducible way (Fig. 2C and D). Stages of different diameters were easily counted and distinguished for dimensions, morphology and staining intensity. AO staining showed an intense fluorescence, associated with stages including merozoites, sporozoites and plasmodia. The emission was sufficient to distinguish single merozoites or their crown around

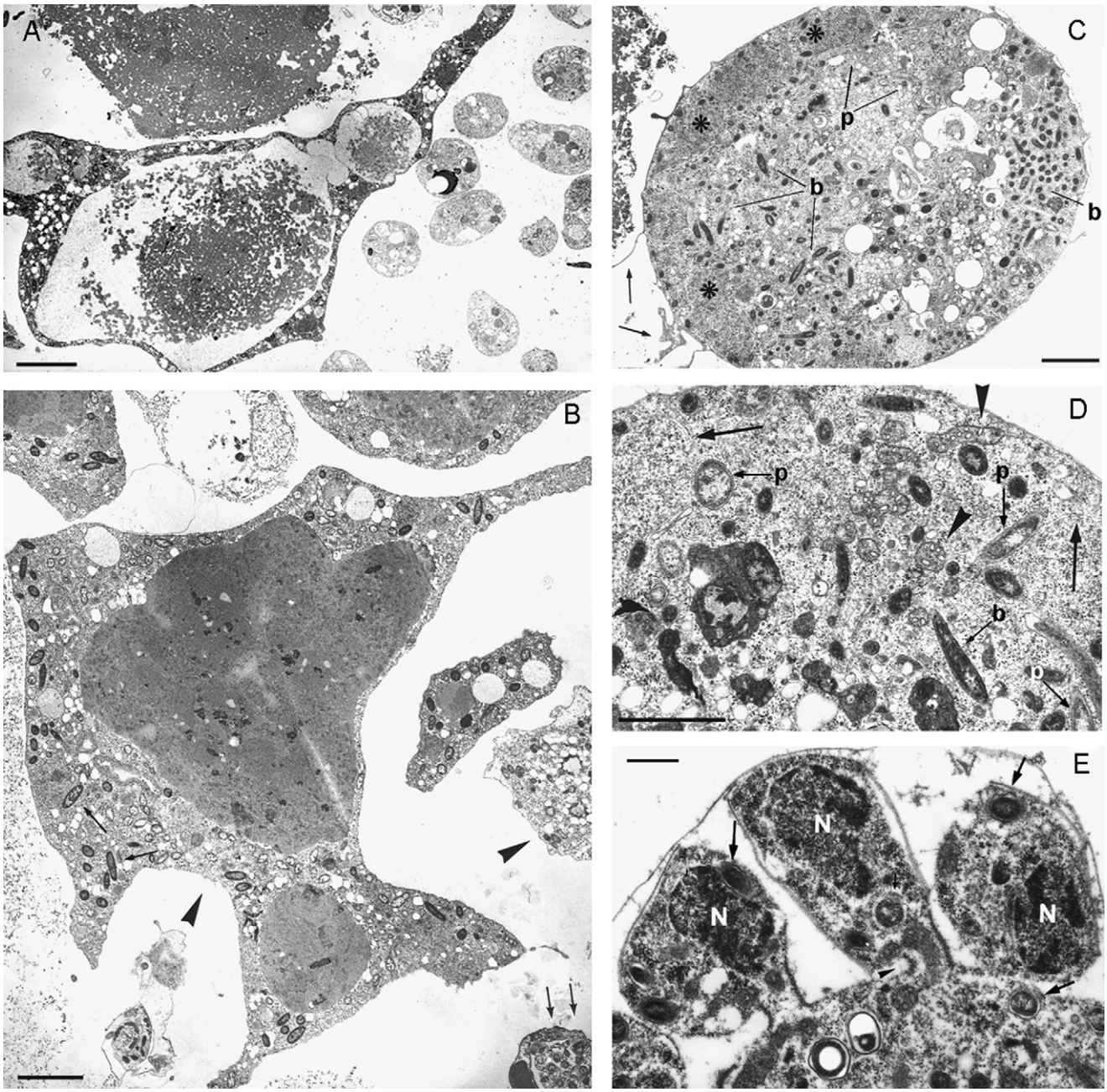

Fig. 4. TEM images of plasmodial stages of *Cardiosporidium cionae* from the pericardial body of *Ciona intestinalis*. Maturing plasmodia (A, B, arrowheads) show internal divisions (B), elongated protrusions and endosymbiotic bacterial cells (B, arrows). Early merogonic stages within haemocytes are also visible (B, paired arrows at bottom right). At a more advanced stage plasmodia show differentiation of early merozoites in peripheral areas (C, asterisks), vesiculated mitochondria (D, arrowheads), apicoplasts (C, p; D, p) bacterial cells (C, b; D, b). The areas of merozoite differentiation are delimited by a double membrane (D, larger arrow). Mature merogonic stages within the pansporoblastic membrane differentiate as merozoites, separated by an isthmus from the plasmodium (E). The merozoites show electron-dense nuclei (N), endosymbiotic bacterial cells (small arrows) and vesiculated mitochondria, migrating from the merogonic plasmodium (arrowhead). Scale bars: A = 5 μm; B = 3.6 μm; C = 2.5 μm; D = 1.0 μm; E = 0.5 μm.

sporonts, with a sufficient background contrast. The staining was specific, since only the cells of *C. cionae* were visible in epifluorescence on the background (Fig. 1D), improving detection efficiency when compared to transmitted light alone (Fig. 1C).

Ultrastructure

TEM sections revealed a correspondence of *C. cionae* ultrastructure with details of plasmodial stages visible in LM and epifluorescence. Further developmental details were observed for plasmodia, which were also found in sections of *C. intestinalis* haemocytes (Fig. 5B–D). TEM also showed the occurrence of an apicoplast and an electron-dense organelle, considered as a putative bacterial endosymbiont, both inside cleaving merozoites (Fig. 6A and B) and within the plasmodial cores (Fig. 5A). They appeared as elongated, electron-dense bodies 0.2–0.3 μm wide, often found in the peripheral regions in more differentiated stages (Figs 3–5).

Immature plasmodia were free in the pericardial cavity, with uniform and poorly differentiated electron-dense nuclear areas. Free plasmodia varied from fusiform to

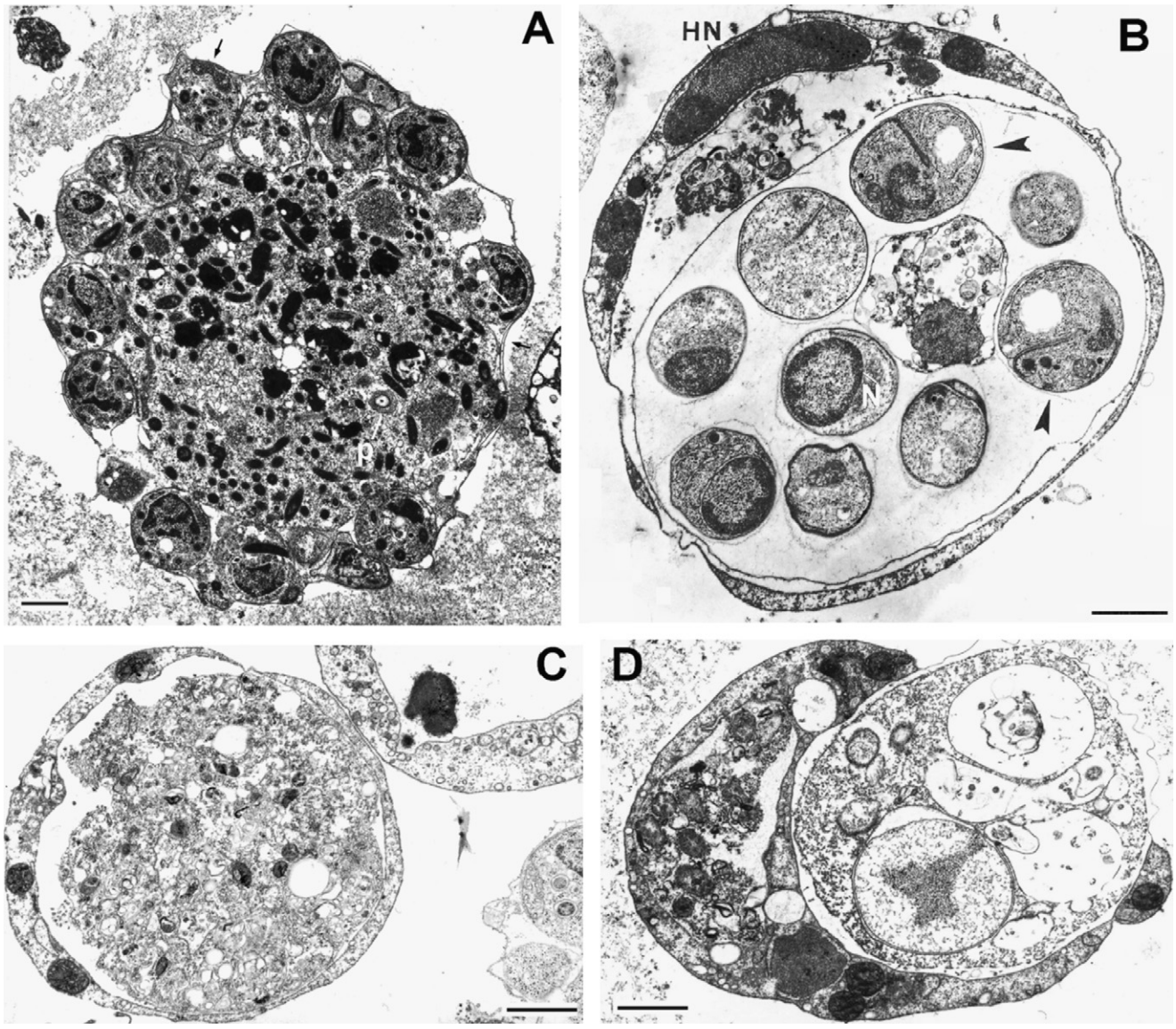

Fig. 5. Merogony of *Cardiosporidium cionae* in a more advanced differentiation phase, showing cleavage of merozoites from sporogonial plasmodia within the pericardial body of *Ciona intestinalis* (A) or in haemocytes of the same host (B). The host haemocyte still retains a laterally compressed nucleus (HN). Merozoites around the sporogonial plasmodium are enclosed by a double membrane (A, arrows). Merozoites of *C. cionae* enclosed within haemocytes of *C. intestinalis* (B, arrowheads) show a self-bending process, a vesiculated single mitochondrion, rhoptries, and a nucleus (N). Haemocyte cells parasitized by *C. cionae* also show a lateral compression of the cell nucleus and mitochondria during the early stages of plasmodium division (C, D). Scale bars: A–D = 1 μm.

irregular in shape (Fig. 3A–D) and showed a central area of varying electron density. Large numbers of putative endosymbiotic rods were observed at this stage (Figs 3E and 4B, D). A progressive reduction of the electron-dense material was observed among plasmodia at different maturing stages. In some sections the electron-dense central cores also showed internal budding (Fig. 3C and D). In stages considered as more advanced, this area was delimited by a membrane and embedded in more electron-transparent material, free of the putative endosymbionts, which clustered at the plasmodium periphery (Figs 3E and 4A, D).

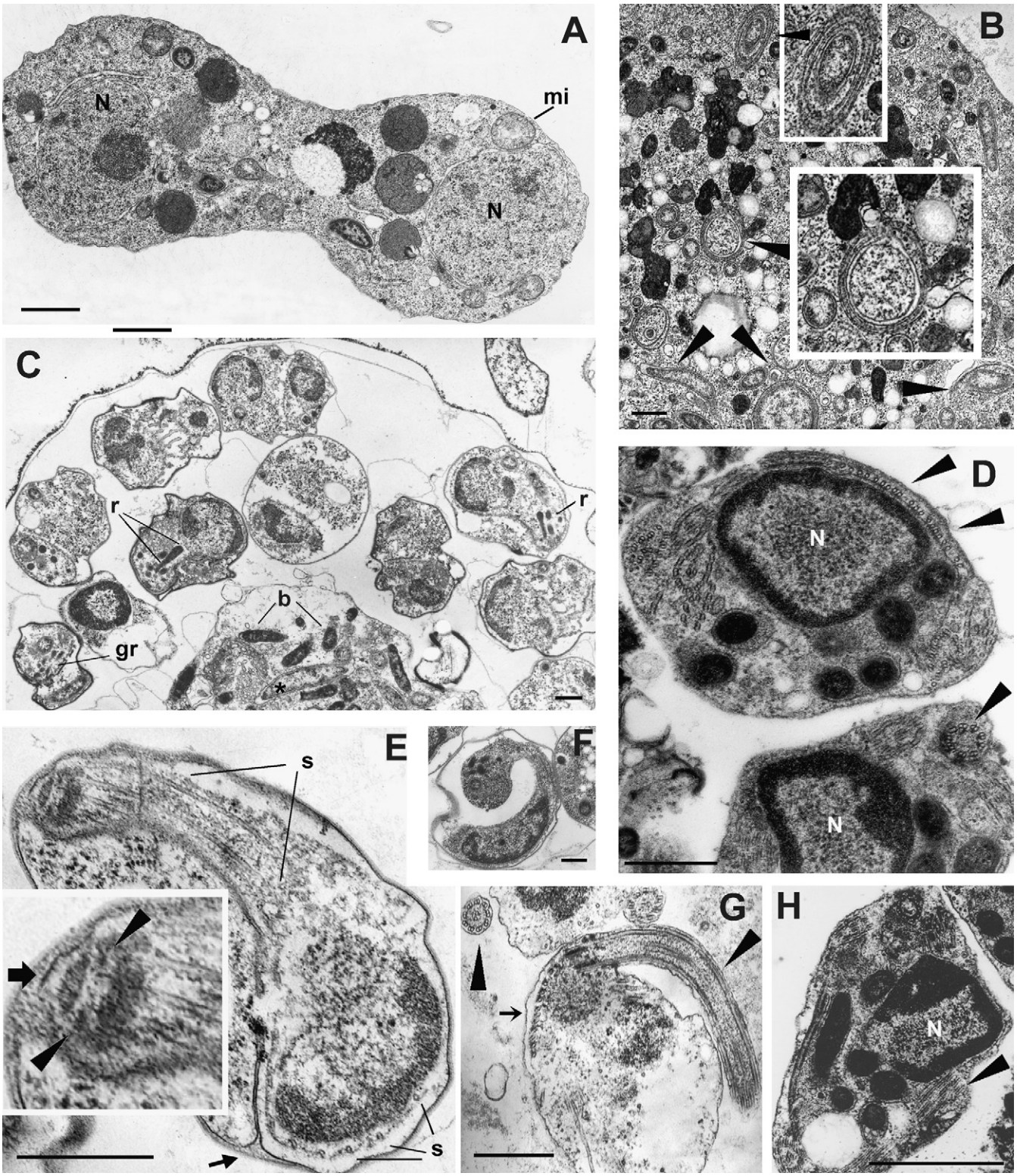

The merozoites cleaved in the outer sporont periphery (Figs 4E, 5A, B and 6C). Budding merozoites showed irregular and elongated mitochondria, rich in vesicles, frequently observed at the periphery of early differentiating sporonts (Figs 4D, E and 5A). The merozoites were encircled within an apparent double outer membrane distinct from the pansporoblastic membrane (Figs 4E and 5A, B).

Plasmodia and merogonic stages with differentiating merozoites were also observed inside *C. intestinalis* haemocytes (Fig. 5B–D). The haemocyte appeared almost destroyed by the parasite, as shown by the presence of residual degenerating material, including the nucleus, laterally compressed at the cell periphery, whereas the plasmodia showed a central residual body with degenerating material and merozoites (Fig. 5B). Two distinct membrane layers separated the merozoites from the host cell. Self-folding cells provided with electron-dense rhoptries were also observed at this stage within plasmodia (Fig. 5B). The self-folding process was observed also in advanced merogonic stages formed at the periphery of plasmodia free in the pericardial body, and appeared consistent with a structural reorganization of the merozoite cell (Figs 6C, E, F and 7A–D).

Electron-dense rhoptries were visible, at more advanced developmental stages, in the apical merozoite regions, showing a spherical body 125–240 nm wide, narrowing to give rise to a duct (Fig. 7A and D). Rhoptries were flanked by 60–100 nm wide electron-dense granules (Fig. 7B–D and H) and micronemes (Fig. 7E and F).

Different stages of the *C. cionae* life-cycle were observed within the same pericardial bodies, and the parasite development appeared asynchronous. Apart from developing plasmodial stages and merozoites, TEM sections also showed secondary merogonic stages of *C. cionae* in division, characterized by a high density of ribosomes, nuclei with nucleoli surrounded by vesiculated mitochondria and other spherical, electron-dense refractile bodies (Fig. 6A).

Apicoplasts, 540–850 nm in diameter and characterized by four concentric membrane layers, were observed in plasmodial (Figs 6B and 7I) and merogonic stages (Fig. 7G). They appeared as elongated electron lucent rods (Fig. 6C) or as organelles provided with a series of four concentric layers (Fig. 6B, insets) or whorls (Fig. 7G and I). The elongated apicoplasts were distinguished from the putative endosymbiotic bacteria because of a lower electron density and staining intensity (Figs 4D and 6C).

Mature merozoitic stages also showed subpellicular microtubules 20–30 nm in diameter, arranged longitudinally within the cell, spanning from the nuclear area and converging towards the apical region, located on the opposite side (Fig. 6E). Subpellicular microtubules were also present in maturing sexual stages (Fig. 6D–H), as well as in sporocysts (Fig. 7H) and appeared to be involved in the cell organization and bending process. Merozoites showed the presence of an apical prominence of the plasma membrane with a central darker zone and a simple polar ring, towards which the microtubules converged (Fig. 6E, inset). Flagellated sexual stages were observed to develop within plasmodia as well as free in the pericardial space (Fig. 6D and G–H). The flagella of male microgametes displayed in section the typical 9 + 2 structure (Fig. 7G). The sporocyst showed the occurrence, in transverse and longitudinal sections, of an external trilaminar wall (Fig. 7G and H). Peripheral subpellicular microtubules were also visible in longitudinal section in the sporocyst cell periphery, as well as in an internal region, as a result of the coming together of the cell tips, due to the self-bending process. In this area, an internal loop was also visible, derived from replication of the cell membrane and flanked by parallel subpellicular microtubules. Rhoptries and granules were also present in the sporocyst in an area distinct from that of the nucleus and the vesiculated mitochondrion (Fig. 7H).

Prevalence

C. cionae was observed for more than a decade in *C. intestinalis* specimens collected in different areas of the Gulf of Naples. It was found in 2 consecutive years in specimens collected at Castellammare di Stabia, with highest prevalence levels observed in October–November (Fig. 8). By the end of the sampling period almost all specimens showed pericardial bodies with plasmodial stages. Similar parasitism levels were

Fig. 6. Secondary merogonic stage of *Cardiosporidium cionae* in a dividing process (A) showing abundance of ribosomes, two separated nuclei (N) with nucleoli surrounded by vesiculated mitochondria (mi), and spherical refractile bodies. Apicoplasts in the plasmodial stage (B arrowheads) showing the four membrane organization in transverse and diagonal sections (insets). Plasmodia in a more advanced stage of merozoite differentiation (C), showing folding merozoitic cells provided with rhoptries (r) and granules (gr), electron-dense bacterial endosymbionts (b) and electron-lucent apicoplast (asterisk). Sections of microgamonts (D, H) showing the nuclear area (N), the arrangement of the subpellicular and flagellar microtubules (arrowheads), as well as electron-dense putative endosymbionts. Maturing merozoite (E) showing subpellicular microtubules (s) converging towards the apical region with two apical microtubules (inset, arrowheads) and a simple polar ring with an apical prominence of the plasma membrane (inset, bold arrow). The cell folding process gives rise to an empty space (arrow) adjacent to the nuclear region, which is flanked by the subpellicular microtubules (s). Longitudinal section of maturing merozoites showing the "C" self-bending process (F). Flagellated sexual stages found free in the pericardic space (G) showing the flagellar 9 + 2 microtubule organization (arrowheads), and subpellicular microtubules (arrow). Scale bars: A, B = 1 μm; C–H = 0.5 μm.

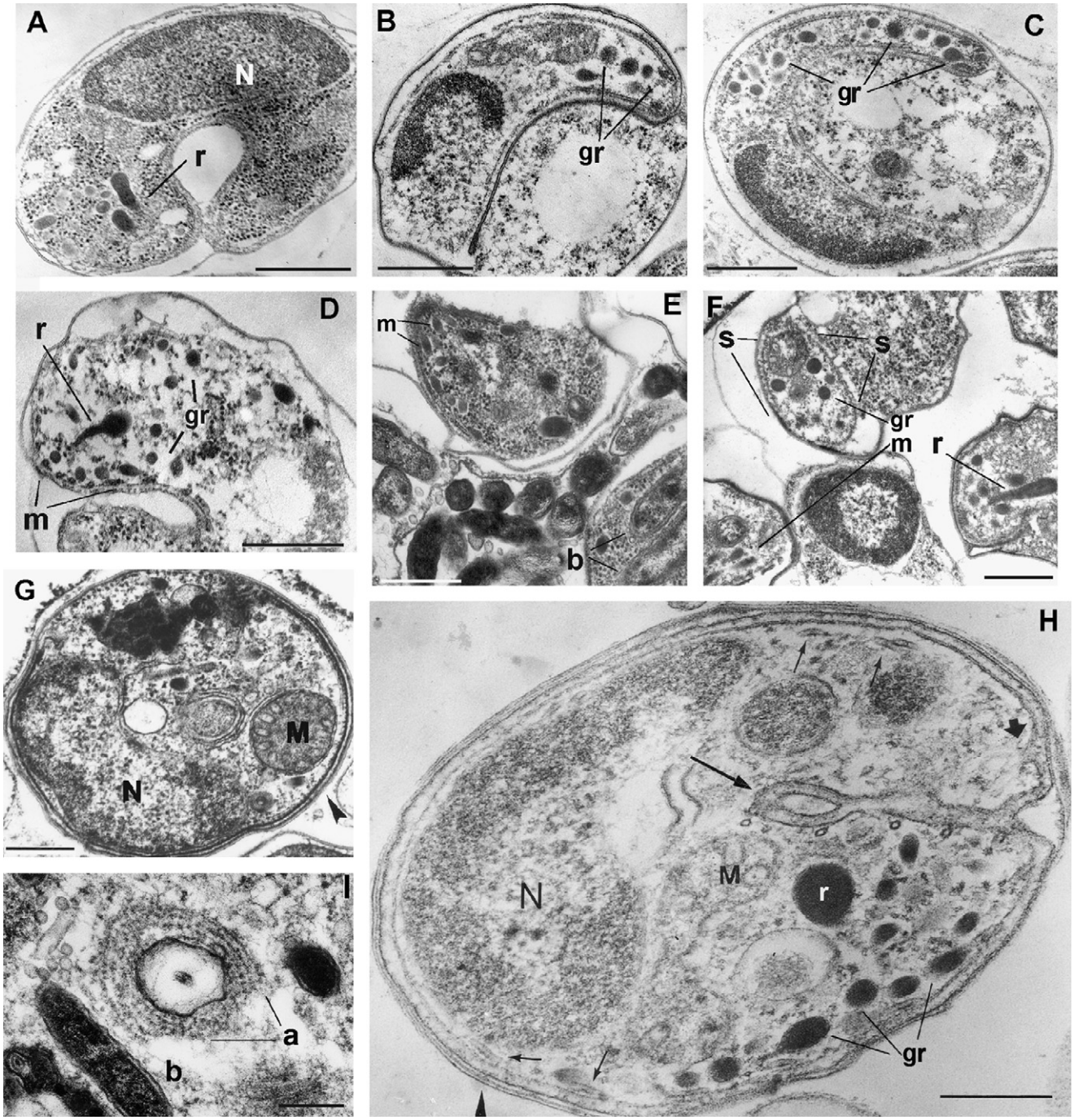

Fig. 7. Maturing merogonic stages of *Cardiosporidium cionae* showing organelles and the cell self-bending process (A–F). Rhoptries (r) and micronemes (m) are visible at this stage, opposite to the nuclear region (N) and surrounded by subpellicular microtubules (s) converging towards the cell apex (E, F). Bacteria-like cells (b) were observed both within and in proximity to maturing merozoites cleaving from the plasmodia (E). Bacterial cells were also found within the plasmodium (I), flanking concentric apicoplast-like structures (a). The sporocysts show, in transverse (G) and longitudinal sections (H), an external trilaminar wall (arrowheads). Peripheral subpellicular microtubules (H, small arrows) are visible in longitudinal section. An internal loop (large arrow) is also visible, originating from the bending of the cell membrane (bold arrow), and flanked by a set of parallel subpellicular microtubules. Rhoptries (r) and granules (gr) are visible in sporocyst regions distinct from the area of the nucleus (N) and the vesiculated mitochondrion (M). Scale bars: A–H = 500 nm; I = 250 nm.

also found in the following year for specimens collected from the same place, with prevalence ranging from 77.8% to 55.5% by the end of October. Specimens of *C. intestinalis* collected at Lago Fusaro showed the presence of pericardial bodies, but no plasmodia were found within the material examined.

Phylogenetic position

The primers used for PCR amplification yielded a fragment of 1921 bp (GenBank accession: EU052685).

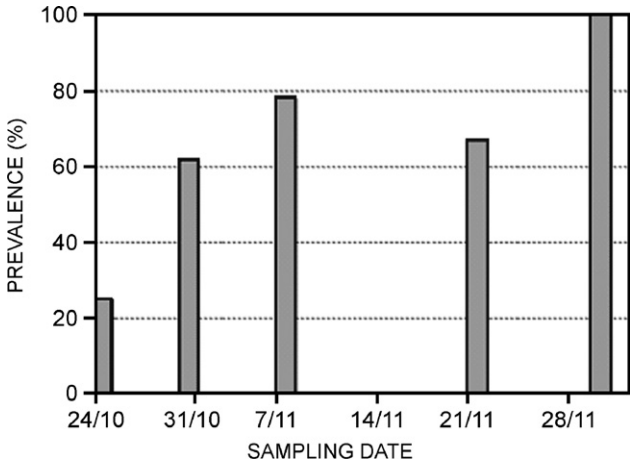

Fig. 8. Time series prevalence data for the plasmodial stages of *Cardiosporidium cionae* in specimens of a population of *Ciona intestinalis* collected from Castellammare di Stabia (Italy).

Content in G + C was 43.47% (A: 27.69%; C: 18.22%; G: 25.25% and T: 28.84%). BLAST search with the sequence obtained showed highest nucleotide identities with fragments of the rSSU sequences of *Cytauxzoon* spp. (92–94%), *Adelina dimidiata* (93%), *Babesia poelea* (93%) and *Toxoplasma gondii* (92%), as well as with *Cystoisospora* spp. (92%) and *Isospora* (92%). Close similarity levels (90–93%) were also scored for accessions AF238264, AF238265 and AF238266 from other unidentified marine organisms (Toller et al. 2001). Alignment with closest known species showed a region of 66 nucleotides located at position 1644 (Fig. 9), characterized by higher T (42.4%) and lower C (10.6%) content. The region appeared unique for *C. cionae*, since no match was found in any other sequence available for BLAST search.

Neighbour-joining phylogenetic trees, based on either the Kimura three-parameter distance or the Jukes and Cantor substitution per site calculations, always located *C. cionae* within other apicomplexan clades, placing the genus *Cardiosporidium* as a further evolutionary radiation amid closest piroplasm parasites of the genera *Theileria*, *Cytauxzoon* and *Babesia* (Fig. 10).

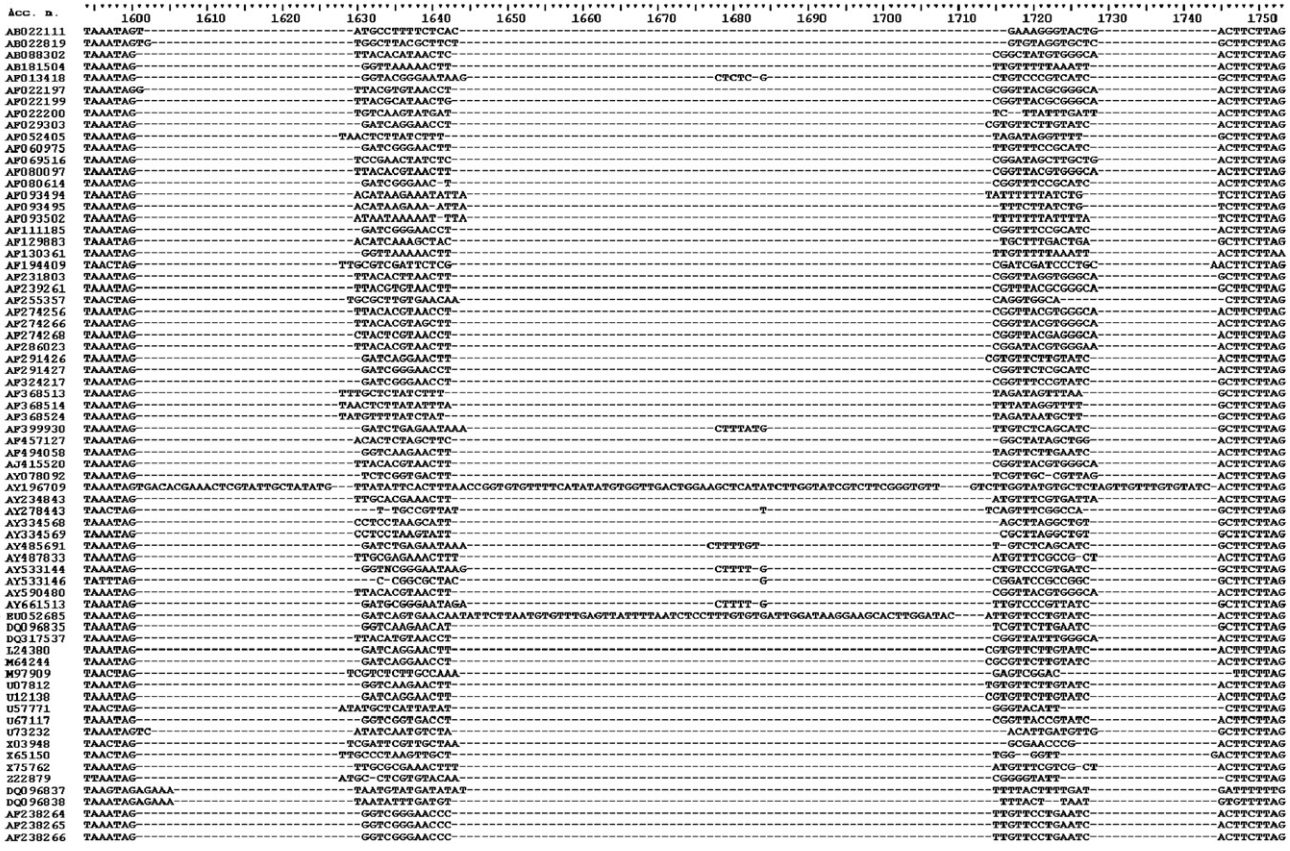

Fig. 9. Alignment of the PCR amplified product with the SSU rDNA accessions of representatives of Apicomplexa and related taxa, showing the nucleotide region specific for *Cardiosporidium cionae* (GenBank accession: EU052685; position 1644 of alignment) and corresponding insertions found in *Selenidium terebellae* (AY196709).

Description

Genus *Cardiosporidium* Van Gaver and Stephan, 1907 (Apicomplexa: Piroplasmida)

(emended from Van Gaver and Stephan [1907] and Scippa et al. [2000])

Diagnosis: Parasitic in ascidians. Plasmodial stages, sporogonial merozoitic phases and free merozoites present in the heart cavity and in the host pericardial body. Plasmodial stages and merogonial phases also within haemocytes. Merozoites differentiating with a double membrane distinct from the resting plasmodial

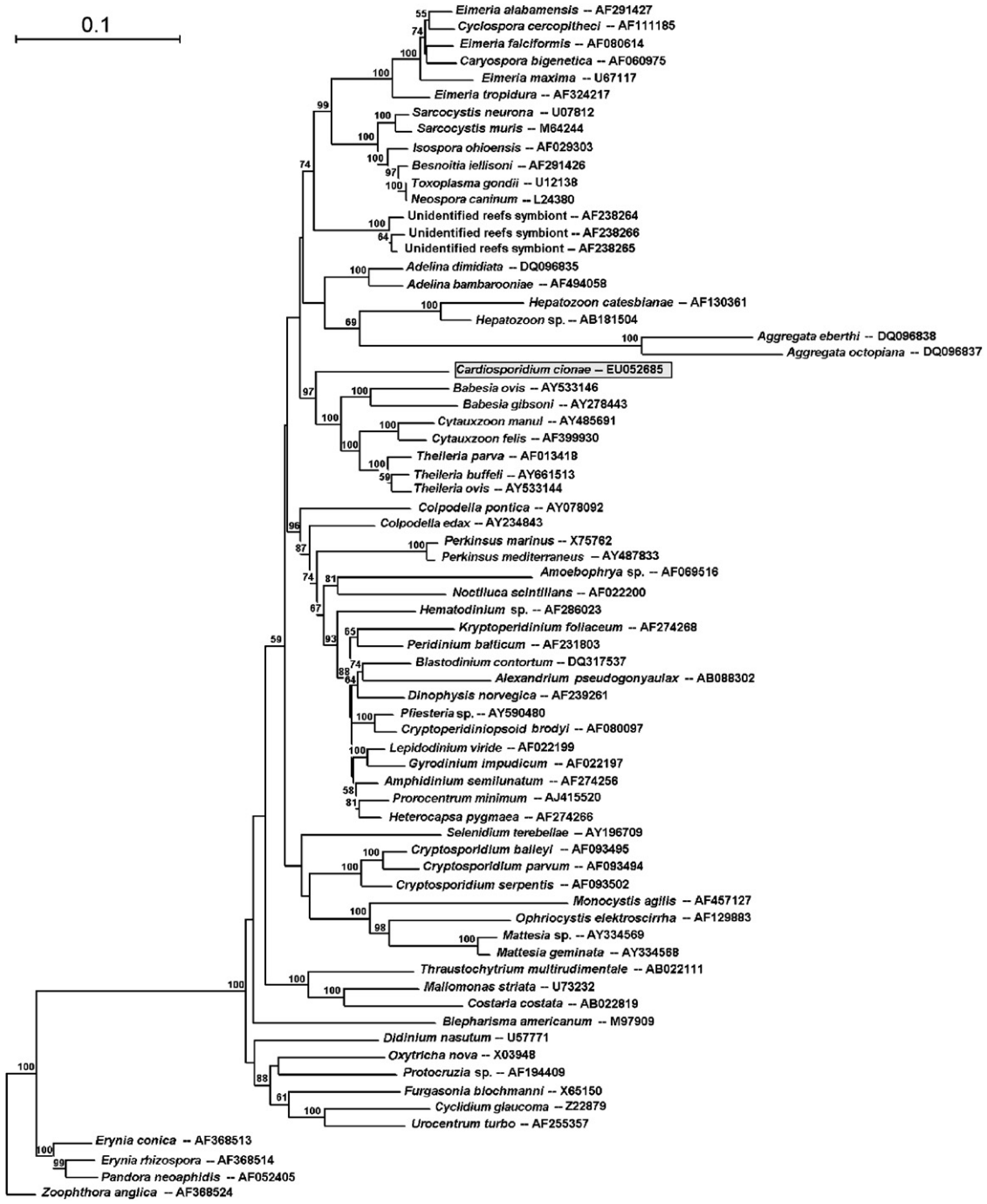

Fig. 10. Rooted Neighbour-joining tree showing the phylogenetic relationship of *Cardiosporidium cionae*, based on the amplified SSU product and the corresponding GenBank accessions of other Apicomplexa and related taxa (accession numbers are shown after species names). The tree was constructed using the Jukes and Cantor distance values with 100 bootstraps. The bar shows the rate of nucleotide divergence, the numbers at nodes show the percent of bootstrap resamplings (higher than 50%), supporting the shown topology.

membrane, cleaving and then separated by an isthmus from the sporont and finally free within its periphery. Merozoites showing, during late merogonic stages, self-bending to a "C" shape, rhoptries, subpellicular microtubules and a polar ring. Sexual stages formed in the same host, motile male microgametes provided with two flagella. Mitochondria vesiculated. Apicoplast present. Gamonts develop within the same host.

Type species: *Cardiosporidium cionae* (Figs 1–7)

Cardiosporidium cionae Van Gaver and Stephan, 1907 (Figs 1–7)

With characters of the genus. So far only found in *C. intestinalis* L.

Plasmodial stages (Figs 1, 2B–D, 3 and 4A–D): Fusiform, at a more mature stage provided with extensions and filamentous protrusions, free in the pericardial body and parasitic in the haemocytes of the ascidian. Plasmodia yielding merogonic phases with subsequent production and release of merozoites in the heart cavity and in the host pericardial body. Merogony phases also occurring within haemocytes of *C. intestinalis*.

Merozoites (Figs 4E and 5B): Differentiating merozoites released within peripheral spaces of plasmodia or in the host pericardial body. Merozoites characterized, during late merogonic stages, by an apical prominence of the plasma membrane, with a central electron-dense zone and a simple polar ring.

Type host: *Ciona intestinalis* L. (Tunicata).

Geographic locality: From specimens of the ascidian *Ciona intestinalis* collected at Castellammare di Stabia, Gulf of Naples, Italy.

Prevalence: 60–100% by October–November.

Sporulation: Merogonic stages in plasmodia free within the pericardial cavity, in plasmodia within the host pericardial body and within haemocytes.

Etymology: Sporozoan from the heart of *Ciona*.

Remarks: Putative endosymbiotic rod-shaped bacteria and apicoplasts present in plasmodia and merozoites.

Transmission: Need for or nature of vector unknown.

Type specimens: Holotype permanent slide n. MCSNVR/Pr/1 deposited at Museo Civico di Storia Naturale, Verona, Italy. Paratype slide n. MCSNVR/Pr/2 deposited at Museo Civico di Storia Naturale, Verona, Italy; second paratype slide deposited at Museo Nacional de Ciencias Naturales (CSIC), Madrid, Spain.

Discussion

Nucleotide and ultrastructural data obtained herein support the validation of the species *C. cionae* and its placement among the Apicomplexa. Maximum nucleotide identity scores observed for the BLAST sequences closest to the product obtained from *C. cionae* were never higher than 94%, supporting *Cardiosporidium* as a genuine, valid genus, representative of a new phylogenetic radiation in Piroplasmida. Molecular methods proved to be informative enough to identify cryptic species and species divergence within piroplasms (Conrad et al. 2006; Criado-Fornelio et al. 2004) and the placement of the organism in question is reinforced by TEM and LM observations. Ultrastructural data showed that the multiplication of *C. cionae* is of the schizogony type (Morrissette and Sibley 2002), and that the parasite undergoes sexual and asexual development in the same host. These observations fit with those reported in the original description of *C. cionae,* carried out by light microscopy (Van Gaver and Stephan 1907).

The association with the pericardial body cells and the development of merogonic stages inside haemocytes showed that *C. cionae* is a blood parasite. The rSSU sequence and the inferred phylogenetic position coherently placed *C. cionae* with other piroplasms like *Cytauxzoon*, *Babesia* and *Theileria*. In comparison to other Apicomplexa (Dubey et al. 1998), TEM observations of *C. cionae* showed a reduced apical complex, mainly organized in an apical central dark area, and a polar ring. Although the apical complex is a distinctive trait of Apicomplexa, its structural organization varies, and in some cases it is reduced, e.g. in non-motile *Theileria* sporozoites, in which both the conoid and micronemes are absent (Shaw 2003). The merozoites of *C. cionae* showed other typical apicomplexan organelles like rhoptries and micronemes, electron-dense granules and subpellicular microtubules (Preiser et al. 2000), evident in transverse and longitudinal sections of developing merozoites, or in sexual stages (Fig. 6D, E, G and H).

Ultrastructural details of electron-lucent organelles in *C. cionae*, including their elongated shape, their dispersion in multiplicative plasmodial stages and the electron-transparent interior, support their identification as an apicoplast. The organelle appeared to be of the secondary type, as a multi-membrane compartment with varying shapes representative of different sectors, and shared similarities with apicoplasts observed in TEM sections of other Apicomplexa, including the occurrence of tubular whorls (Fig. 7I) (Köhler 2005; Maréchal and Cesbron-Delauw 2001; Striepen et al. 2000; Van Dooren et al. 2005; Waller and McFadden 2005; Wilson and Williamson 1997). In Apicomplexa, an elongated apicoplast organization is found in late maturation of schizonts, giving rise, in connection with mitochondria, to a spatially branched extranuclear arrangement (Waller and McFadden 2005). The plastids replicate before schizogony and the encoded genes have a functional role (Wilson and Williamson 1997). In TEM sections of *C. cionae* (Fig. 6B and insets) this arrangement produced the appearance of clustered plastids, which should be considered at this stage as

part of an unique, elongated and multi-branched organelle. Plastids in *Toxoplasma gondii* are involved in the formation of the parasitophorous vacuole, whereas in *P. falciparum* and *P. berghei* they are related to the survival of the parasite blood stages or to the development of both sexual and asexual forms, respectively (Sullivan et al. 2000). During development of sexual stages, the female macrogamete is the only parent transmitting an apicoplast (Wilson and Williamson 1997). As preliminary evidence supporting the identification of an apicoplast in *C. cionae*, a fragment of approximately 964 bp was amplified during this study by PCR. The sequenced product (data not shown) was obtained from the same DNA as that which yielded the SSU amplicon used for phylogenetic analysis, through a set of primers constructed on the *Toxoplasma gondii* plastid Tu elongation factor (NCBI sequence NC_001799, complete apicoplast genome).

The electron-dense, elongated structures considered as putative endosymbionts, recognized in schizonts of *C. cionae* and distinct from the apicoplast because of their higher electron density, have no homologues in the closest apicomplexan genera, but are well known in ciliates (Fokin et al. 1996; Görtz 1983, 2001; Vannini et al. 2004). In *C. cionae* the structures were often observed as electron-dense bacterium-like bodies in budding schizonts (Figs 3B, D, E, 4C, D, 5A and 6C) and also within merozoites and male sexual stages (Fig. 6D and H). Further investigations are needed, however, to identify these elements as endosymbiotic bacteria of *C. cionae*. There are, however, suggestive clues for a putative relationship of Apicomplexa with some endosymbiotic bacteria. In *Babesia bovis* an extrachromosomal rSSU was identified, showing only a weak association with the mitochondrial and plastid homologues. Several features of the amplified product of *B. bovis* were consistent with an eubacterial origin and appeared closely related to those of a similar organelle-like rSSU, obtained from *Plasmodium falciparum* (Gozar and Bagnara 1995). *Cryptosporidium parvum* is also considered as the recipient of several genes of eubacterial origin, which are expressed and developmentally regulated during the parasite life-cycle (Huang et al. 2004).

The divergence of Apicomplexa from dinoflagellates, which pre-dates the appearance of vertebrates, is estimated to have occurred during the Precambrian (Escalante and Ayala 1995) through a transition of early predators, probably archigregarines or predatory protalveolate flagellates, towards intracellular parasitism (Leander et al. 2003b; Cavalier-Smith and Chao 2004; Kopečná et al. 2006). The Phylum Apicomplexa includes obligate parasites of medical and veterinary importance for man and higher vertebrates, and ultrastructural or DNA data are available for several haemoparasites. Little is known, however, about apicomplexan parasites of non-vertebrate species (Kopečná et al. 2006). The clade of which *C. cionae* is a member may prove informative not only as a new evolutionary lineage of haemocyte parasites, but also because of the phylogenetic position of tunicates which have been recently re-considered as simplified chordates, rather than as the closest organisms to chordate ancestors (Chourrout et al. 2006). In this regard, the presence in ascidian haemocytes of a piroplasm-like species may support the hypothesis of a possible ''retrograde'' evolution of Tunicata (Chourrout et al. 2006).

The host group may represent a distinctive diagnostic character for the genus *Cardiosporidium*. Considering the paucity of data about apicomplexans parasitic in non-vertebrate species and the position of tunicates, the *C. cionae* rSSU data enlarge our knowledge about putatively ''missing'' Apicomplexa or cryptic evolutionary radiations. It is possible that representatives of closely related taxa, often difficult to identify or present in low abundance or in specific environmental niches (Toller et al. 2001), could prove more informative about both the host range and the evolutionary paths of early Apicomplexa, as well as on the emergence of parasitism in Alveolata (Kopečná et al. 2006). In this regard, the 66 bp nucleotide region at position 1644, which appears unique for the rSSU of *C. cionae* (Fig. 9), may have a practical use in providing a suitable basis for the design of molecular probes or specific PCR primers. This insertion was mirrored only by an insertion of 64 bp present in the same region of sequence AY196709 obtained from *Selenidium terebellae* (Leander et al., 2003b), which is flanked by two further shorter insertions which were absent in *C. cionae* (Fig. 9). A low similarity (45.39%) was found, however, between the two fragments. It is worth noting the utility of this specific fragment, as molecular probes or PCR primers specific for this region may be used for amplification and detection of *C. cionae* or other closely related, cryptic species from other ascidian hosts or populations (Choi et al. 2006), as well as to study the parasite ecology or life-cycle inside its host.

The nature and origin of the pericardial body in *C. intestinalis* remains obscure. It was proposed that either parasitism by *C. cionae* and factors related to cellular degenerative processes were involved in a host inflammatory response occurring at the pericardial tissue level, yielding cell remnants and debris, aggregating to form the pericardial body (Scippa et al. 2000). However, lack of detection of parasitic stages of *C. cionae* in specimens of *C. intestinalis* derived from the Lago Fusaro population, which do possess pericardial bodies, suggests that further experimental data in controlled conditions are required to determine the origin and relationships of this structure in *C. intestinalis*.

The AO staining procedure appeared more specific than other techniques (e.g. toluidine blue) previously

used for examination of pericardial bodies (Scippa et al. 2000). The stain specificity was useful during the prevalence studies, allowing fast identification and assessment of prevalence in *C. intestinalis* and, in general, in the study of parasitism. Coupled with PCR, it may prove useful in identifying the parasite infection entry route and sites of development in the host.

In conclusion, both phylogenetic and ultrastructural analyses support the assignment of *C. cionae* to the piroplasm clade of Apicomplexa. For a complete understanding of its life-cycle, an experimental approach based on tests on healthy and artificially infected hosts, carried out in controlled conditions, is required. Since known piroplasms are vector-transmitted, the identification of the infective stage of the parasite, together with its putative transmission biology and the occurrence of possible vectors should also be investigated. No data are available thus far on the transmission process of *C. cionae*. Possible entry routes are through feeding (by ingestion of infective sporocysts), by trans-epithelial infection, or by infection during the host larval stage, due to the partial opening of the pericardial cavity which occurs during this stage. A possible hypothesis is that, as for isopods which are intermediate hosts of fish hemogregarines (Davies and Nico 2001), transmission could occur through some aquatic vector, e.g. copepods which are frequently found in the branchial basket tissues or externally on the tunic of ascidians (Ohishi and O'Reilly 2004; Ohishi 2006).

Acknowledgements

The authors gratefully thank Dr. Carmela Izzo for TEM preparations and Dr. A. Toscano and Mr. Ciro Zazo, Stazione Zoologica "Anton Dohrn", Naples, for sampling and specimen collection. Research partially funded by CNR, Agenzia 2000.

References

Cavalier-Smith, T., Chao, E.E., 2004. Protalveolate phylogeny and systematics and the origins of Sporozoa and dinoflagellates (phylum Myzozoa nom. nov.). Eur. J. Protistol. 40, 185–212.

Choi, D.L., Jee, B.Y., Choi, H.J., Hwang, J.Y., Kim, J.W., Berthe, F.C.J., 2006. First report on histology and ultrastructure of an intrahemocytic paramyxean parasite (IPP) from tunicate *Halocynthia roretzi* in Korea. Dis. Aquat. Organ. 72, 65–69.

Chourrout, D., Delsuc, F., Chourrout, P., Edvardsen, R.B., Rentzsch, F., Renfer, E., Jensen, M.F., Zhu, B., de Jong, P., Steele, R.E., Technau, U., 2006. Minimal ProtoHox cluster inferred from bilaterian and cnidarian Hox complements. Nature 442, 684–687.

Conrad, P.A., Kjemtrup, A.M., Carreno, R.A., Thomford, J., Wainwright, K., Eberhard, M., Quick, R., Telford III, S.R., Herwaldt, B.L., 2006. Description of *Babesia duncani* n. sp. (Apicomplexa: Babesiidae) from humans and its differentiation from other piroplasms. Int. J. Parasitol. 36, 779–789.

Criado-Fornelio, A., Gónzalez-del-Río, M.A., Buling-Saraña, A., Barba-Carretero, J.C., 2004. The "expanding universe" of piroplasms. Vet. Parasitol. 119, 337–345.

Darzynkiewicz, Z., 1990. Differential staining of DNA and RNA in intact cells and isolated cell nuclei with acridine orange. Meth. Cell Biol. 33, 285–298.

Darzynkiewicz, Z., Kapuscinski, J., 1990. Acridine orange: a versatile probe of nucleic acids and other cell constituents. In: Melamed, M.R., Lindmo, T., Mendelsohn, M.L. (Eds.), Flow Cytometry and Sorting, second ed. Wiley, New York, pp. 291–314.

Davies, A.J., Nico, J.S., 2001. The life cycle of *Hemogregarina bigemina* (Adelina: Haemogregarinidae) in South African hosts. Folia Parasitol. 48, 169–177.

Dubey, J.P., Lindsay, D.S., Speer, C.A., 1998. Structures of *Toxoplasma gondii* tachyzoites, bradyzoites, and sporozoites and biology and development of tissue cysts. Clin. Microbiol. Rev. 11, 267–299.

Eisenman, E.A., Alfert, M., 1982. A new fixation procedure for preserving the ultrastructure of marine invertebrate tissues. J. Microsc. 125, 117–120.

Escalante, A.A., Ayala, F.J., 1995. Evolutionary origin of *Plasmodium* and other Apicomplexa based on ribosomal-RNA genes. Proc. Natl. Acad. Sci. USA 92, 5793–5797.

Felsenstein, J., 1985. Confidence limits on phylogenies: an approach using the bootstrap. Evolution 39, 783–791.

Fernandez, M., 1906. Zur kenntnis des perikardcörpers einiger ascidien. Jenaische Zeitsch. Naturwiss 41, 1–18.

Fokin, S.I., Brigge, T., Brenner, J., Görtz, H.-D., 1996. *Holospora* species infected the nuclei of *Paramecium* appear to belong into two groups of bacteria. Eur. J. Protistol. 32 (Suppl. 1), 19–24.

Görtz, H.-D., 1983. Endonuclear symbionts in ciliates. Int. Rev. Cytol. 14, 145–176.

Görtz, H.-D., 2001. Intracellular bacteria in ciliates. Int. Microbiol. 4, 143–150.

Gozar, M.M.G., Bagnara, A.S., 1995. An organelle-like small subunit ribosomal RNA gene from *Babesia bovis*: nucleotide sequence, secondary structure of the transcript and preliminary phylogenetic analysis. Int. J. Parasitol. 25, 929–938.

Hall, T.A., 1999. BioEdit: a user-friendly biological sequence alignment editor and analysis program for Windows 95/98/NT. Nucl. Acids Symp. Ser. 41, 95–98.

Huang, J., Mullapudi, N., Lancto, C.A., Scott, M., Abrahamsen, M.S., Kissinger, J.C., 2004. Phylogenomic evidence supports past endosymbiosis, intracellular and horizontal gene transfer in *Cryptosporidium parvum*. Genome Biol. 5, R88.

Kalk, M., 1970. The organization of the tunicate heart. Tissue Cell 2, 99–118.

Kawamoto, F., 1991. Rapid diagnosis of malaria by fluorescence microscopy using light microscope and interference filter. Lancet 337, 200–202.

Kimura, M., 1980. A simple method for estimating evolutionary rates of base substitutions through comparative study of nucleotide sequences. J. Mol. Evol. 16, 111–120.

Köhler, S., 2005. Multi-membrane-bound structures of Apicomplexa: I. The architecture of the *Toxoplasma gondii* apicoplast. Parasitol. Res. 96, 258–272.

Kopečná, J., Jirku, M., Oborník, M., Tokarev, Y.S., Lukeš, J., Modrý, D., 2006. Phylogenetic analysis of coccidian parasites from invertebrates: search for missing links. Protist 157, 173–183.

Jukes, T.H., Cantor, C.R., 1969. Evolution of protein molecules. In: Munro, H.N. (Ed.), Mammalian Protein Metabolism. Academic Press, New York, pp. 21–123.

Leander, B.S., Clopton, R.E., Keeling, P.J., 2003a. Phylogeny of gregarines (Apicomplexa) as inferred from small-subunit rDNA and β-tubulin. Int. J. Syst. Evol. Microbiol. 53, 345–354.

Leander, B.S., Harper, J.T., Keeling, P.J., 2003b. Molecular phylogeny and surface morphology of marine aseptate gregarines (Apicomplexa): *Selenidium* spp. and *Lecudina* spp. J. Parasitol. 89, 1191–1205.

Leander, B.S., Kuvardina, O.N., Aleshin, V.V., Mylnikov, A.P., Keeling, P.J., 2003c. Molecular phylogeny and surface morphology of *Colpodella edax* (Alveolata): insights into the phagotrophic ancestry of apicomplexans. J. Euk. Microbiol. 50, 334–340.

Maréchal, E., Cesbron-Delauw, M.-F., 2001. The apicoplast: a new member of the plastid family. Trends Pl. Sci. 6, 200–205.

McDonald, K., 1984. Osmium ferricyanide fixation improves microfilament preservation and membrane visualization in a variety of animal cell types. J. Ultrastruct. Res. 86, 107–118.

Millar, R.H., 1953. *Ciona*. L.M.B.C. Memoirs on Typical British Marine Plants and Animals, vol. 35. The University Press of Liverpool, UK, pp. 1–123.

Morrissette, N.S., Sibley, D.L., 2002. Cytoskeleton of apicomplexan parasites. Microbiol. Mol. Biol. Rev. 66, 21–38.

Mpoke, S.S., Wolfe, J., 1997. Differential staining of apoptotic nuclei in living cells: application to macronuclear elimination in *Tetrahymena*. J. Histochem. Cytochem. 45, 675–683.

Ohishi, S., 2006. Two species of *Botryllophilus* (Copepoda: Cyclopoida) living in compound ascidians, and a revision of female morphotype A of the genus. J. Crust. Biol. 26, 23–47.

Ohishi, S., O'Reilly, M.G., 2004. Redescription of *Haplostoma eruca* (Copepoda: Cyclopoida: Ascidicolidae) living in the intestine of *Ciona intestinalis* from the Clyde estuary, Scotland. J. Crust. Biol. 24, 9–16.

Ormières, R., 1964. Recherches sur les sporozoaires parasites des tuniciers. Vie Milieu 15, 823–946.

Payne, D., 1988. Use and limitations of light microscopy for diagnosing malaria at the primary health care level. Bull. World Health Org. 66, 621–626.

Preiser, P., Kaviratne, M., Khan, S., Bannister, L., Jarra, W., 2000. The apical organelles of malaria merozoites: host cell selection, invasion, host immunity and immune evasion. Micr. Inf. 2, 1461–1477.

Roule, M.L., 1884. Recherche sur les ascidies simples des côtes de Provence (Phallusiadées). Ann. Mus. Hist. Nat. Mars., Zool. Tome II.

Saitou, N., Nei, M., 1987. The neighbor-joining method: a new method for reconstructing phylogenetic trees. Mol. Biol. Evol. 4, 406–425.

Scippa, S., Izzo, C., 1996. An ultrastructural study of the hemocytes of the pericardic body in the ascidian *Ciona intestinalis*. Acta Zool. 77, 283–286.

Scippa, S., Ciancio, A., De Vincentiis, M., 2000. Observation on the ultrastructure of an apicomplexan parasite of *Ciona intestinalis*. Eur. J. Protistol. 36, 85–88.

Shaw, M.K., 2003. Cell invasion by *Theileria* sporozoites. Trends Parasitol. 19, 2–6.

Striepen, B., Crawford, M.J., Shaw, M.K., Tilney, L.G., Seeber, F., Roos, D.S., 2000. The plastid of *Toxoplasma gondii* is divided by association with the centrosomes. J. Cell Biol. 151, 1423–1434.

Sullivan, M., Li, J., Kumar, S., Rogers, M.J., McCutchan, T.F., 2000. Effects of interruption of apicoplast function on malaria infection, development, and transmission. Mol. Biochem. Parasitol. 109, 17–23.

Thompson, J.D., Higgins, D.G., Gibson, T.J., 1994. CLUSTAL W: improving the sensitivity of progressive multiple sequence alignment through sequence weighting, positions-specific gap penalties and weight matrix choice. Nucl. Acid Res. 22, 4673–4680.

Toller, W.W., Rowan, R., Knowlton, N., 2001. Zooxanthellae of the *Montastraea annularis* species complex: patterns of distribution of four taxa of *Symbiodinium* on different reefs and across depths. Biol. Bull. 201, 348–359.

Van de Peer, Y., De Wachter, R., 1997. Construction of evolutionary distance trees with TREECON for Windows: accounting for variation in nucleotide substitution rate among sites. Comput. Appl. Biosci. 13, 227–230.

Van Dooren, G.G., Marti, M., Tonkin, C.J., Stimmler, L.M., Cowman, A.F., McFadden, G.I., 2005. Development of the endoplasmic reticulum, mitochondrion and apicoplast during the asexual lifecycle of *Plasmodium falciparum*. Mol. Microbiol. 57, 405–419.

Van Gaver, F., Stephan, P., 1907. *Cardiosporidium cionae*, sporozoaire nouveau parasite du corps pericardique de *Ciona intestinalis*. C.R. Soc. Biol. Paris 62, 556–557.

Vannini, C., Rosati, G., Verni, F., Petroni, G., 2004. Identification of the bacterial endosymbionts of the marine ciliate *Euplotes magnicirratus* (Ciliophora, Hypotrichia) and proposal of 'Candidatus *Devosia euplotis*'. Int. J. Syst. Evol. Microbiol. 54, 1151–1156.

Waller, R.F., McFadden, G.I., 2005. The Apicoplast: a review of the derived plastid of apicomplexan parasites. Curr. Issues Mol. Biol. 7, 57–80.

Wilson, R.J.M., Williamson, D.H., 1997. Extrachromosomal DNA in the Apicomplexa. Microbiol. Mol. Biol. Rev. 61, 1–16.